Graefe's Arch Clin Exp Ophthalmol (1987) 225:189–197

Graefe's Archive
for Clinical and Experimental
Ophthalmology

Canthaxanthin retinopathy

An investigation by light and electron microscopy and physicochemical analysis

B. Daicker[1], K. Schiedt[2], J.J. Adnet[3], and P. Bermond[4]

[1] Universitäts Augenklinik, Mittlere Strasse 91, CH-4056 Basel, Switzerland
[2] F. Hoffmann-La Roche & Co. Ltd., Basel, Switzerland
[3] Laboratoire Pol Bouin, Centre Hospitalier Universitaire, Reims, France
[4] Hôpitaux de Reims, Reims, France

Abstract. The eyes of a patient with canthaxanthin retinopathy were obtained at autopsy and examined by light and electron microscopy. Various tissues of one eye were also studied by physicochemical methods. Morphologically, there were red, birefringent, lipid-soluble crystals in the inner layers of the entire retina. They were particularly large and numerous perifoveally, where they were also clinically visible, but they also occurred frequently in a ring-shaped form peripherally and, less frequently, equatorially. The crystals were located in a spongy degeneration of the inner neuropil, where atrophy of the inner parts of the Müller cells was noticed. The compound isolated from the retina was identical with synthetic canthaxanthin according to mass and proton-resonance spectroscopy. Quantitatively, the retina contained up to 42 μg canthaxanthin per gram of tissue besides a minor amount of other carotenoids. Of the other tissues of the eye, only the ciliary body contained measurable concentrations of canthaxanthin. From the great number and size of the crystals, on the one hand, and the relatively small amount of isolated canthaxanthin on the other, it was concluded that the crystals presumably represent a canthaxanthin-lipoprotein complex rather than pure canthaxanthin alone. Examination showed that clinically, only the central portion of the canthaxanthin thesaurismosis, where crystals are packed most densely, can be seen.

Introduction

Since 1982, several reports have appeared in the ophthalmological, dermatological, and pharmaceutical literature describing a hitherto unknown central retinopathy with a very characteristic clinical picture (Boudreault et al. 1983; Cortin et al. 1982, 1984; Franco et al. 1985; Hennekes et al. 1985; Metge et al. 1984; McGuiness and Beaumont 1985; Meyer et al. 1985; Philipp 1985; Ros et al. 1985; Rousseau 1983; Saraux and Laroche 1983; Weber et al. 1985a, b; Weber and Goerz 1985, 1986). It is characterized by glistening, golden-yellow crystals deposited in the inner layer of the retina. These deposits may develop until they are 10–14 μm in size (Boudreault et al. 1983; Cortin et al. 1982; Ros et al. 1985) and are located principally in a ring-shaped area between 5° and 10° around the fovea. They are less numerous in the fovea and are seen only exceptionally in the foveola (Cortin et al. 1982). In rare cases they are located nasal to the disc (Metge et al. 1984) or irregularly disseminated in the posterior fundus (B. Daicker 1986, unpublished data) without annular formation. They were found only once in the periphery of the fundus in the inner layer of a retinoschisis (Cortin et al. 1982). The deposits almost invariably occur bilaterally. Unilaterally or with unilateral predominance they are observed only in rare cases (Metge et al. 1984). In certain patients, mainly elderly persons, there were also small hyaline drusen in the retinal pigment epithelium (Boudreault et al. 1983; Cortin et al. 1984; Weber et al. 1985a).

In the fluorescence angiogram the deposits are not visible, and their annular formation sometimes masks the fluorescence of the choroid (Cortin et al. 1982; Franco et al. 1985; Metge et al. 1984; Philipp 1985; Saraux and Laroche 1983). The patients are usually free from functional symptoms. In rare cases the patients complain of a sensation of dazzle or blurred vision (Cortin et al. 1984; Hennekes et al. 1985; Philipp 1985). It is, however, not clear whether these symptoms are related to the deposits. Visual reduction, diplopia, or metamorphopsia are found only in patients with additional eye diseases (Cortin et al. 1984). The color sense is always intact; visual field defects are described by only one author (Ros et al. 1985).

The EOG is normal or subnormal (Boudreault et al. 1983; Metge et al. 1984; McGuiness and Beaumont 1985; Weber et al. 1985b). Dark adaptation is found to be normal (Boudreault et al. 1983) or delayed (Hennekes et al. 1985; McGuiness and Beaumont 1985; Philipp 1985; Weber et al. 1985a). Scotopic vision after exposure to glare is reduced (Hennekes et al. 1985; Weber et al. 1985b). The electroretinogram is described as normal or with b-wave changes (Hennekes et al. 1985; McGuiness and Beaumont 1985; Weber et al. 1985b).

All patients with this retinopathy (82 cases quoted in the literature so far) took preparations[1] containing canthaxanthin (β,β-carotene-4,4′-dione), a reddish carotenoid of the xanthophyll family but, unlike β-carotene, not a precursor of vitamin A. Most preparations also contain β-carotene. They are used for skin pigmentation in vitiligo and for light protection in polymorphous photodermatosis and erythropoietic protoporphyria (Puissant 1984; Ros et al. 1985; Tronnier 1984) or for cosmetic tanning. For the medi-

Offprint requests to: B. Daicker

[1] Phenoro, Apotrin, Orobronze, Brun-utan-sol, Bronzeactive, and Bellacarotin

cal application, the recommended dosages correspond to 45–60 mg canthaxanthin/day. In the cosmetic application, however, higher dosages have been taken.

Whereas medication with β-carotene alone has so far not been found to cause retinal lesions (Poh-Fitzpatrick and Barbera 1984) and the use of the mentioned combined preparations over short periods or at low doses has not led to any clinically manifest retinopathy (A. Huhtala and H. Pitkänen 1985, unpublished data; Meyer et al. 1985b), total doses of over 30 g canthaxanthin in 24 months induced retinopathies in 50% of the patients, and doses over 60 g have infallibly resulted in retinopathy (Metge et al. 1984). The occurrence of retinal deposits depends on the total dose of canthaxanthin and, to a lesser degree, on age (Boudreault et al. 1983; Ros et al. 1985; Weber et al. 1985a). Intraocular hypertension and focal retinal pigment epitheliopathy may act as predisposing factors (Cortin et al. 1984).

Functional disturbances are reversible months after therapy has been terminated, but crystalline deposits in the retina have been found to be irreversible in the observation periods so far possible (Ros et al. 1985; Weber and Goertz 1986). Therefore, the crystals as such are not responsible for the functional disorder. It is not known whether the crystals observed in one case in the corneal endothelium are connected with the retinal deposits (Philipp 1985).

The nature of the retinal deposits is so far not known. We had the opportunity of examining both eyeballs obtained at autopsy of a female patient showing the complete picture of this retinopathy. Histological, ultrastructural, and spectroscopical analyses of the deposits were carried out to elucidate their characteristics.

Material and methods

Both eyeballs of a woman were examined[2] who had died at the age of 72 years after complications during anesthesia. Over the years she had taken a total dose of 1,125 capsules of Phenoro (11.2 g β-carotene, 16.8 g canthaxanthin) as treatment for vitiligo. In a routine examination of her eyes, the ophthalmologist had discovered glistening macular deposits. However, she never complained of any subjective side effects that could possibly have been due to the deposits. The visual functional tests carried out a short time before surgery proved normal for her age.

Figure 1 shows the clinical appearance of the right fundus one year before death. Between this time and the fatal incident the patient had not taken any more carotenoid-containing medication. The cornea of the left eye was removed postmortem for keratoplasty.

Morphological studies

The eyeballs were fixed in 4% buffered formalin (Lillie). After equatorial division into halves, the right globe was inspected under a dissecting microscope, and stereoscopic photographs were made of the retinal lesions in situ and in the excised parts. Portions of the retina from the area of the temporal macula, from the nasal margin of the papilla, from the equator and the region of the ora serrata, as well as corresponding portions of choroid with adhering retinal pigment epithelium, were studied as unstained flat mounts in the light microscope and in polarized light. Frozen sections of the same parts were examined unmodified and after dehydration with alcohol in polarized light and after hematoxylin and eosin, oil red O and Sudan black staining.

Further portions of the retina were embedded in an egg-white sandwich in paraffin and stained with H&E, van Gieson, PAS and PTAH. The same stains were used on the choroid, cornea, and optic nerve. Frozen sections of the anterior and posterior half of the left globe were stained with Sudan black, oil red O, and Sudan IV and paraffin sections with hematoxylin-phloxin-saffron, Masson's trichrome stain, PAS, alcian blue, Masson-Fontana for melanin, Schmorl stain for lipofuscin, Sirius red, and reticulin silver. Small pieces of the central retina were washed in distilled water, crushed between slides and examined by scanning electron microscopy (SEM) after air-drying and gold-coating.

Other portions of the temporal central retina of the right (o.d.) and the equatorial eyeball wall of the left eye (o.s.) were postfixed in phosphate-buffered 2.5% glutaraldehyde and OsO_4, embedded in Epon, and examined in semithin sections by transmission electron microscopy (TEM) after contrasting with lead citrate.

Qualitative and quantitative chemical analyses of carotenoids

The residual retina, choroid, ciliary body, iris, lens, optic nerve, and sclera were subjected to physicochemical analysis. After dissection of the eye, the various parts were again stored in 4% neutral formalin until analysis. The sizes of the remaining retinal parts and of the ciliary body were measured after removal of samples for histopathological examination. The results were calculated for total tissues (Tables 2–4).

Extraction. Prior to analysis the tissues were swabbed with Whatman filter paper and the wet weight determined. After dehydration with approximately double the amount of anhydrous $MgSO_4$, the tissues were homogenized and extracted with reagent grade acetone. The solvent was sucked off through a glass filter and evaporated under a N_2 stream.

VIS spectrophotometry. The residues of the extracts were dissolved in 0.5–2 ml *n*-hexane containing 2%–5% ethanol and their VIS spectra recorded in a Uvikon 810 spectrophotometer.

High-pressure liquid chromatography (HPLC) analysis. Two systems were used: one for the identification of canthaxanthin, separating the all-*trans*- and *cis*-isomers, and a second for the separation of the more polar dihydroxy- and mono-keto-monohydroxy-carotenoids, whereby the *cis*/*trans* isomers eluted as only one peak.

Identification of canthaxanthin from retinal tissue by physical methods

The following physical methods were used for the identification of 1.4 µg all-*trans*-canthaxanthin isolated from retinal tissue by HPLC:

1. ^{1}H-NMR (proton magnetic resonance), 400 MHz, 0.135 ml $CDCL_3$, 100% D, acquisition time 14.5 h.

2. Mass spectroscopy.

[2] Ocular, histological, and ultrastructural examinations of the right eye were performed by author[1], the physicochemical studies of the right eye by author[2], and the histological and ultrastructural studies of the left eyeball by author[3]

Scanning microscope photometric analysis (SMP) of crystals in the retina in situ was compared with synthetic canthaxanthin. Energy-dispersive X-ray analysis (Tracer TN 5500) was performed on the matrix and the crystals of the SEM specimens.

Results

Morphological studies

Macroscopic examination. Externally, there were no pathological findings in the right eyeball; the central part of the vitreous body had undergone vacuolar destruction. After removal of the vitreous body, which was turbid due to fixation, the retina appeared opaque and the fovea was surrounded by an elliptic pink ring 1.5 mm in width and diameters of 5 and 7 mm, respectively. A foveal central area of 2×3 mm diameter was not colored (Figs. 2, 3). No macula lutea could be seen. A crescent-shaped red coloration of the retina extended nasally to the disc. At a distance of 1–2 mm from the ora serrata, the peripheral retina was also tinted red in a circular zone 2.5–3 mm wide. In some places the cystoid degeneration of the outermost retina extended into the zone of coloration (Fig. 4). On higher magnification with the stereomicroscope, the innermost layers of the entire central retina, but in particular the macroscopically red colored areas, were found to contain a great number of glistening yellowish-to-reddish points scattered throughout. Depending on the incidence of the light, some disappeared while others lit up. On macroscopic examination, the majority and largest of the glistening points were located in the red perifoveal ring (Fig. 5), whereas in the peripheral ring they were less frequent and much smaller. The uncolored foveolar area was completely free.

Histology. Light microscopy of flat mounts of unstained fixed retina show innumerable reddish, birefringent crystals with dichroism. They are punctiform, rod-shaped or flake-like, the largest also being plate-like and oblong with punched-out corners (Figs. 7, 8). They are 4–25 µm in size and usually randomly scattered or in piles. They are arranged paracentrally in rows between the nerve fibers (Fig. 6). Infrequently they also lie in apposition to small vessels (Fig. 9).

The red tint of the retina, visible macroscopically, is obviously due to these red crystals. In the frozen section, these red birefringent crystals are found exclusively within the innermost layers of the retina, extending from the limiting membrane to the inner nuclear layer. They are not sudanophilic and were eluted by high-grade alcohol. No crystaline deposits were observed within the choroid or the retinal pigment epithelium (Fig. 11).

In the paraffin sections, isolated amyloid bodies are found in the paracentral to peripheral nerve fiber layer. Between the ganglion cell layer and the internal limiting membrane there is a spongy region formed by irregular, sometimes septated, optically empty lacunae, which is pronounced perifoveally and less pronounced peripherally. This tissue dissociation is on a larger scale than usually takes place postmortem disintegration. The lacunae sometimes cause indentation of the blood vessels (Fig. 12).

The retina, choroid, and optic nerve present no abnormalities with the stainings used in the paraffin section. The rather poorly pigmented retinal epithelia contain a moderate amount of lipofuscin centrally and a greater amount peripherally.

By *SEM*, piles of polygonal or whetstone-shaped crystals, often toothed and clearly laminated, can be observed (Fig. 10a, b).

The *TEM* images are seriously impaired by artifacts due to postmortem decay and the unfavorable original fixation. Examination of the central nerve fiber and ganglion cell layer reveals partly confluent and septated lacunae, which are large at the center and small peripherally. They are mostly empty or have some granular content or convoluted membranes. Due to the artifacts it is not possible to decide whether the lacunae are invariably surrounded by membranes or whether they are located intra- and/or extracellularly. The penicillate feet of the Müller cells are strikingly slender and bizarrely branched. Their footplates are dehiscent and do not form the usual continuous layer towards the basal membrane (Fig. 13) (Foos 1972; Jakobiec 1982). Some of the lacunae are apposed to the unchanged basal membrane either by immediate contact or via a thick, fragmented osmiophilic membrane (Figs. 13, 14). Melanin granules are rare in the retinal pigment epithelium, but there is a large number of lipofuscin and melanolipofuscin granules.

Physicochemical studies

The habitus of the VIS spectrum of the lipid extracts gave strong evidence of the type of carotenoid. From the extinction at λ max, the carotenoid content could be calculated on the basis of an extinction coefficient (E 1%/1 cm) of 1970 for canthaxanthin and 2000 for other xanthophylls.

The following carotenoids were identified by HPLC according to their retention times in comparison with those of the corresponding authentic synthetic compounds: canthaxanthin (*β,β*-carotene-4,4′-dione), 4-oxo-*β,β*-caroten-4′-ol, *β,β*-carotene-4,4′-diol and zeaxanthin. Xanthophyll esters were possibly present in samples 4, 5, 12, and 13 (Table 1) but were disregarded because of the minute quantities of total carotenoids in these samples, whose saponification had been avoided.

The analyzed eye tissues (total tissue minus excised pieces for morphological study), their wet weights, total carotenoid content, and concentrations are listed in Table 1. Table 2 shows that in the various retinal tissue samples, canthaxanthin was the main pigment, occurring in concentrations of 17–42 µg/g tissue.

In the retina, a total of 8.6 µg carotenoids was found, 7.8 µg of which was canthaxanthin. The ratios of 93/7 and 91/9 for *trans/cis* canthaxanthin in retinal samples 2 and 3, and of 72/28 in the tanning agent Orobronze and in the pharmaceutical preparation Phenoro, respectively, suggest that the all-*trans*-isomer may be deposited more readily in the retina. The ^{1}H-NMR spectrum of the isolated all-*trans*-canthaxanthin was identical to that of synthetic canthaxanthin, and the mass spectrum of the isolated canthaxanthin exhibited the molecular ion of 564, which is consistent with the molecular weight of canthaxanthin ($C_{40}H_{52}O_2$). The SMP spectrum of the crystals in the retina was approximately identical and its absorption maximum exactly identical with the corresponding data of synthetic canthaxanthin. Energy dispersive X-ray analysis showed a much higher calcium and phosphorus content at the site of the crystals than in the surrounding tissue.

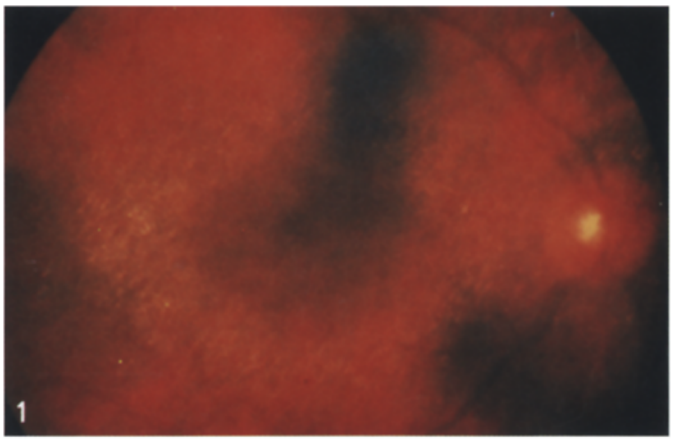
1

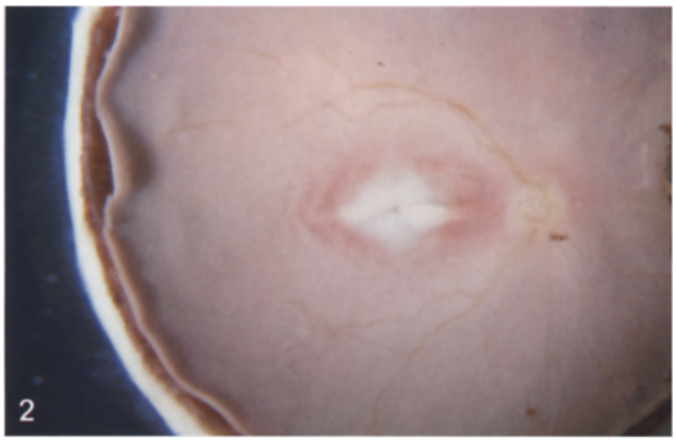
2

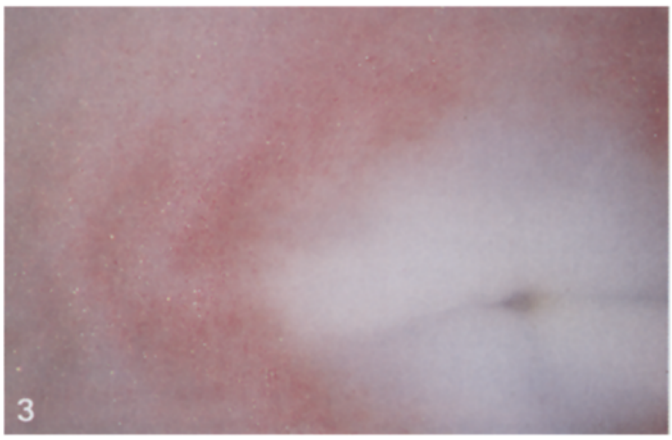
3

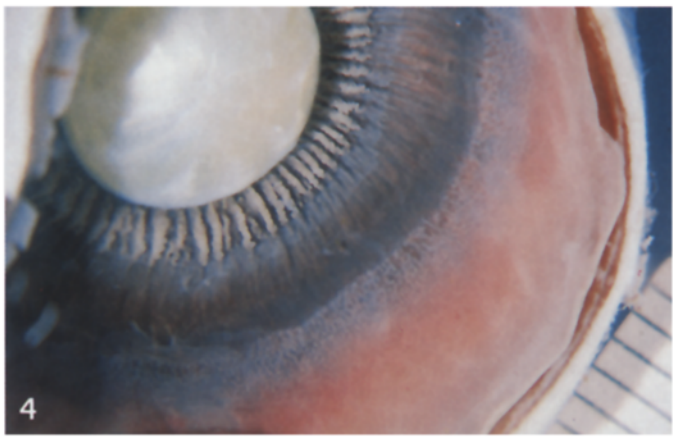
4

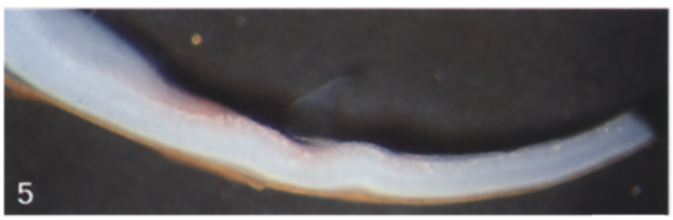
5

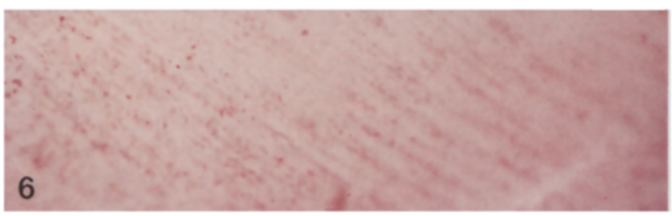
6

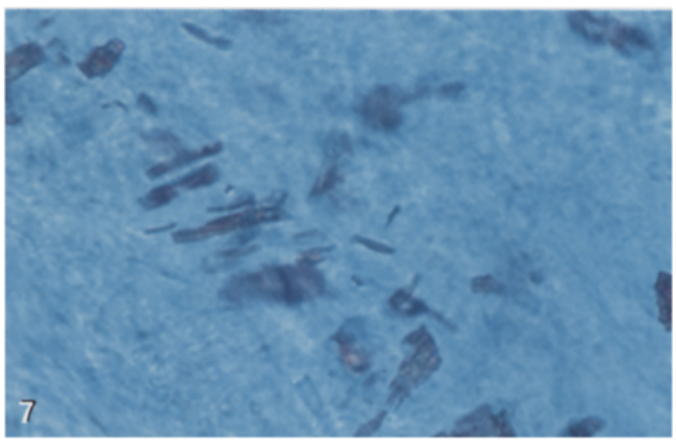
7

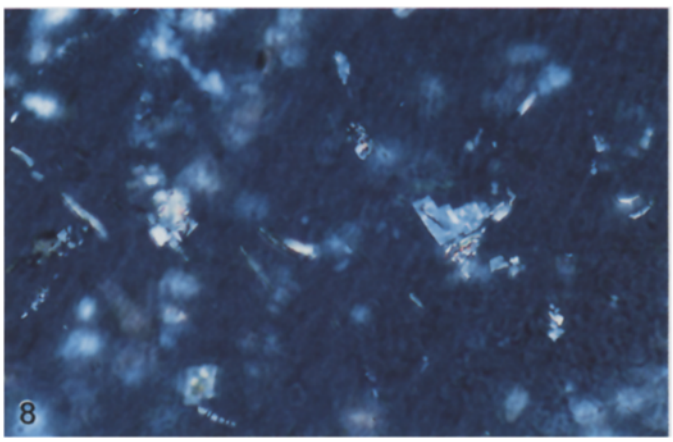
8

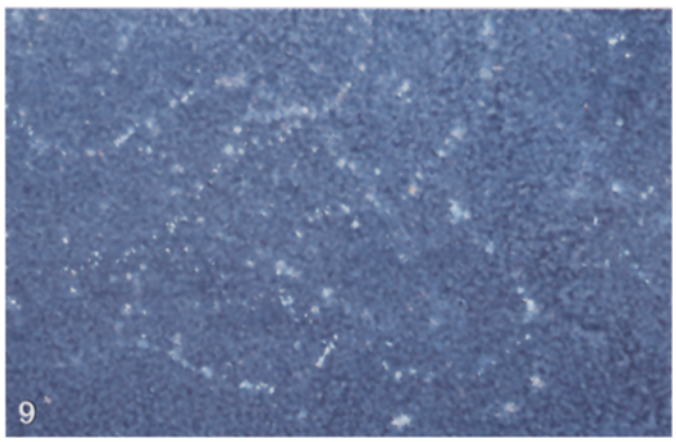
9

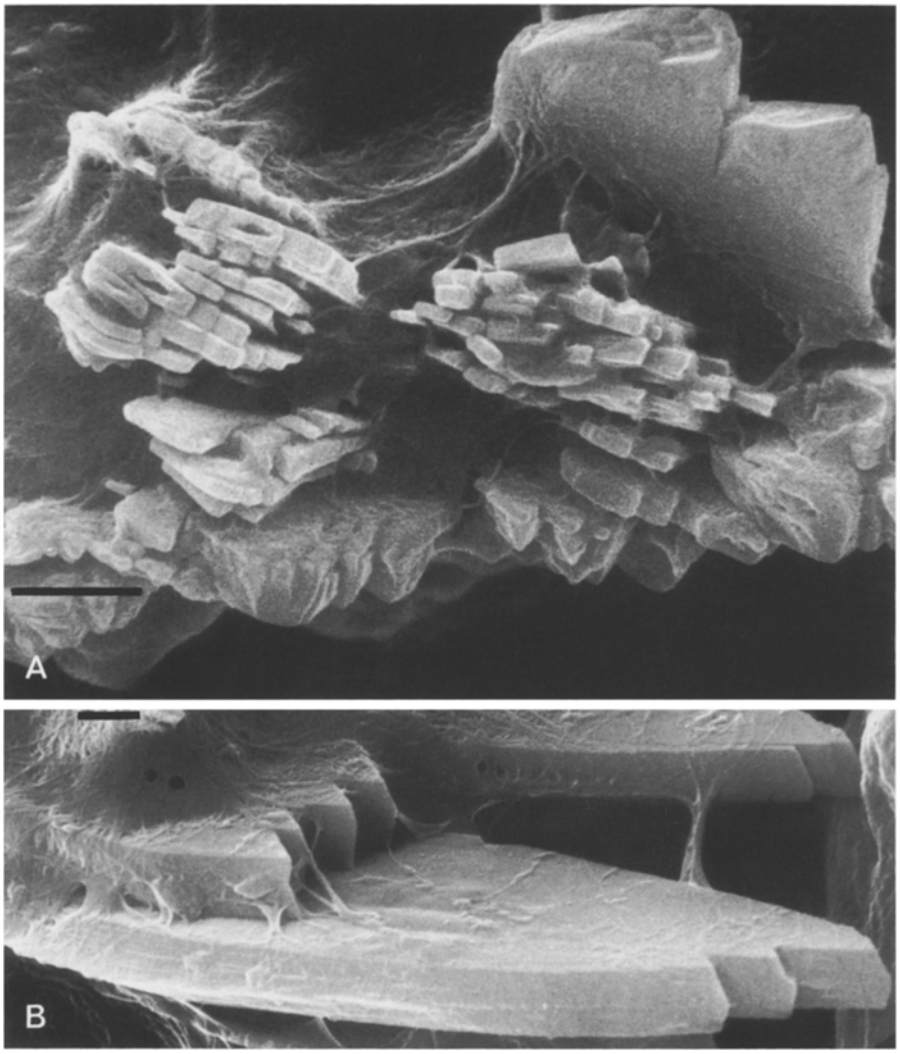

Fig. 10. **A** Piles of crystal plates. **B** Saw-toothed ends and laminated side of the crystals. (SEM; bar = 1 μm)

Fig. 1. Clinical appearance of the right fundus 1 year before death. Glistening crystals are seen in a perifoveal ring-shaped zone

Fig. 2. Ring-shaped red coloration around the fovea. Opacification of the retina and foveal folds are postmortem and fixation artifacts. Autopsy finding (o.d., × 1.9)

Fig. 3. Detail from Fig. 2. Glistening crystals in the inner layer of the red ring. (× 8.7)

Fig. 4. Red-tinted peripheral retina. Autopsy finding (o.d., × 1.9)

Fig. 5. Perpendicular section through central retina shows the coloration and crystals of the inner retinal layers (o.d., × 8.7)

Fig. 6. Rows of red crystals between the nerve fibers. Flat, unstained whole retinal mount. (o.d., × 29)

Fig. 7. Different sizes and forms of the red crystals. Flat, unstained whole mount. (o.d., × 290)

Fig. 8. Birefringency of the crystals in the retina. Unstained whole mount. (o.d., Pol. × 290)

Fig. 9. Deposition of crystals on retinal vessels. Unstained whole mount (o.d., Pol. × 73)

Table 3 is a compilation of the carotenoid contents and concentrations of the other eye tissues (ciliary body, peripheral choroid, posterior choroid, and pigment epithelium). These parts contain carotenoids in lower concentrations (2–10 μg/g tissue). Canthaxanthin as the major pigment was found only in the ciliary body (86%). In the choroid and pigment epithelium the reduction products of canthaxanthin, 4-oxo-β,β-caroten-4′-ol, and β,β-carotene-4,4′-diol were present as the main carotenoids.

In Table 4 the carotenoid content and concentration of the lens, cornea, and sclera are listed. Canthaxanthin was not detected in these tissues. The iris contained no carotenoids at all.

Although the carotenoid content in these tissues was very low, it still lies within the range of the values discribed for lutein and zeaxanthin as macular pigments (Bone et al. 1985).

Discussion

Our morphological studies confirm the clinical assumption that the glistening deposits in the retina represent crystals located in the inner layers of the retina. In the outer retina,

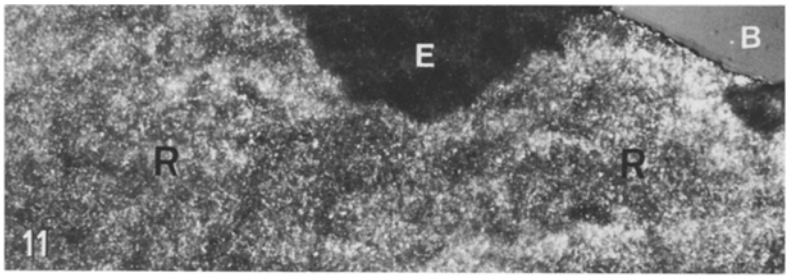

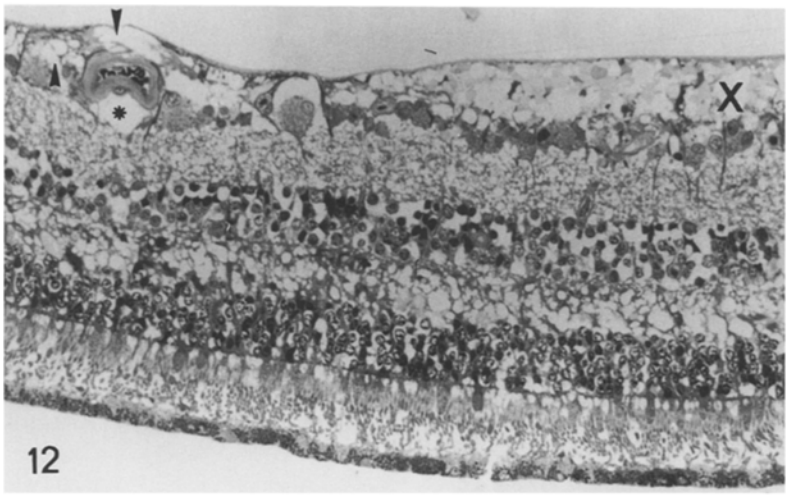

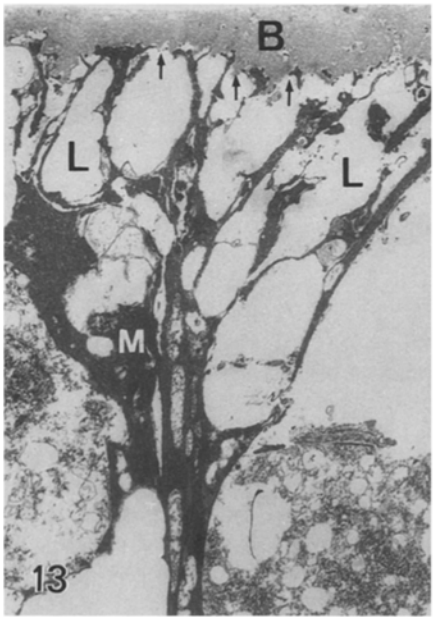

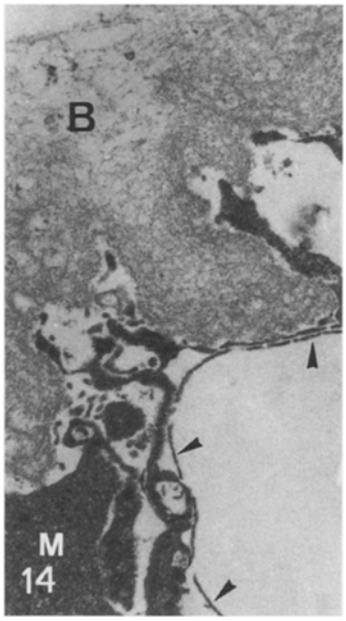

Fig. 11. Top view of a flat mounted unstained equatorial retina (*R*) and pigment epithelium (*E*). *B*, Background. Myriads of birefringent crystals in the retina only. (o.d., ×31)

Fig. 12. Parafoveal retina. Spongy degeneration of the nerve fiber and ganglion cell layer (*X*). Septated lacunae (*arrowhead*). Paravascular lacuna (*). Epon, semifine section. (o.d., ×220)

Fig. 13. Bizarre splitting of shrunken, dark inner processes of Müller cell (*M*) by empty small lacunae (*L*). Gaps (↑) between the footplates of the cell. Basal membrane of the retina (*B*) is intact. (TEM; o.d., ×2500)

Fig. 14. A segmented membrane coats some of the lacunae (*arrowheads*). *M*, Müller cell; *B*, basal membrane. (TEM; o.d., ×12000)

in the retinal pigment epithelium and the choroid, no crystals were observed by microscopic examination.

With regard to the topography of the crystalline deposits, there is good agreement between our patient's clinical picture of the retinopathy, and the findings of the postmortem ocular examination under low magnification. Using higher magnifications than those usually available in clinical investigations, we found innumerable minute crystals disseminated throughout the retina, in addition to the known ring-shaped deposits at the posterior pole. The crystals are more numerous paracentrally and peripherally and also larger paracentrally. The peripheral crystals resemble the glistening points of a diffuse snail track (Daicker 1978). The previously known perifoveal ring is thus simply the expression of the particularly great number of large crystals at this site. From these findings it must be concluded that also in vivo the deposits are more massive and extensive than can be ascertained from the ophthalmoscopical and biomicroscopical appearance. Whereas in vivo the crystals are visible solely by the light reflected from their surfaces, the smallest specimens can readily be recognized in unstained tissue mounts by their birefringency. The fact that they are golden in vivo and pink in vitro can be explained by a pleochromism of reflection. The sum of the dissemin-

Table 1. Carotenoid content and concentration in the different tissues of the eye

No.	Tissue	Wet weight[a] (mg)	Total carotenoids (μg)	Carotenoid concentration (μg/g tissue)	Canthaxanthin (HPLC: area %)
1	Macular retina (rest ~ 4/5)	10.1	0.43	43	90
2	Posterior retina (rest ~ 4/5)	73	1.28	17.6	89
3	Peripheral retina (rest ~ 4/5)	153	5.2	34	91
4	Ciliary body	82	0.87	10.6	86
5	Peripheral choroid (rest ~ 9/10)	35	0.11	3.2	39
6	Posterior choroid (rest ~ 9/10)	59	0.15	2.5	6
7	Pigment epithelium	~2	0.04	–	33
8	Lens	162	0.08	0.5	0
9	Cornea	78	0.007	0.09	0
10	Iris	16.3	0	0	0
11	Posterior sclera	554	0.2	0.34	–
12	Anterior sclera	491	0.06	0.13	–
13	Optic nerve	28	0	0	0

[a] Remainder after removal of samples for histopathological examination

Table 2. Carotenoids in the different parts of the retina (total carotenoids found in the retina: 8.6 μg; canthaxanthin: 7.8 μg)

	Central retina (macula)	Posterior retina (without macula)	Peripheral retina
Wet weight and carotenoids (calculated for whole tissue)	Red ring with crystals	Colorless	Red ring with crystals
Wet weight (mg)	12.6	91.2	191
Carotenoids			
Total content (μg)	0.54	1.6	6.5
Concentration in tissue (μg/g)	42.7	17.6	34
Canthaxanthin (HPLC)			
all-*trans*/*cis*[a] ratio, relative (area %)	81/19	93/7	91/9
Canthaxanthin, all-*trans* + *cis*[a] (area %)	90	89	91
4-Oxo-β,β-caroten-4′-ol (area %)	10	7	5
β,β-Carotene-4,4′-diol (area %)	0	4	5

[a] The various *cis*-isomers were not separated

Table 3. Carotenoids in different nonretinal parts of the eye (total carotenoids found in these parts: 1.2 μg; canthaxanthin: 0.8 μg)

	Ciliary body	Peripheral choroid	Posterior choroid	Pigment epithelium
Wet weight and carotenoids (calculated for whole tissue)	Greyish-black	Greyish-black	Greyish-black	Brownish-orange
Wet weight (mg)	81.7	38.9	65.5	2
Carotenoids				
Total content (μg)	0.87	0.12	0.17	0.04
Concentration in tissue (μg/g)	10.6	3.2	2.5	–
Canthaxanthin (HPLC)				
all-*trans*/*cis*[a] ratio, relative (area %)	88/12	90/10	–	–
Canthaxanthin, all-*trans* + *cis*[a] (area %)	86	43	6	33
4-Oxo-β,β-caroten-4′-ol (area %)	3	4	17	7
β,β-Caroten-4,4′-diol (area %)	0	12	53	15
Zeaxanthin (area %)	0	0	2	–
Xanthophyll esters (?) (area %)	7	37	15	20
Not identified (area %)	4	4	7	25

[a] The various *cis*-isomers were not separated

ated red crystals is responsible for the red tint of the retina seen in the postmortem picture. The coloration becomes more evident in the retina opacified by postmortem edema and fixation. There is no evidence that the red colorant is bound to intravitally uncolored crystals only postmortem or by fixation.

According to analysis with the scanning microscope photometer the red coloration of the crystals is due to canthaxanthin. By this method, canthaxanthin could only be detected at the site of the crystals.

The quantities of canthaxanthin extracted from the retina and determined by quantitative spectrophotometric analysis was 8 μg totally, corresponding to tissue concentrations of 17–42 μg/g. From the great number and the size of the crystals on the one hand and from the relatively small amount of isolated canthaxanthin on the other, it was concluded that presumably the crystals represent a canthaxanthin-lipoprotein complex containing Ca and P rather than pure canthaxanthin alone.

According to qualitative and quantitative analysis of the carotenoids in various eye tissues and areas of the retina,

Table 4. Carotenoids in various other parts of the eye (total carotenoids found in these parts: 0.35 μg; canthaxanthin: none)

	Lens	Cornea	Iris	Posterior sclera	Anterior sclera
Wet weight and carotenoids (calculated for whole tissue)	Yellowish-opaque	Colorless opaque	Greyish-black	Whitish/brown	Whitish/brown
Wet weight (mg)	162	87	16.7	554	491
Carotenoids					
Total content (μg)	0.08 0.5	0.007 0.09	0 0	~0.02 0.34	0.06 0.13
Canthaxanthin (HPLC)	0	–			
4-Oxo-β,β-caroten-4′-ol (area %)	10	–		Extracts pooled and saponified: 0.23 μg carotenoids; too much residue for HPLC analysis	
β,β-Carotene-4,4′-diol (area %)	34	–			
Zeaxanthin (area %)	46	–			
Not identified (area %)	10	–			

the carotenoid concentrations in the retina corresponded with the frequency distribution of the crystals and the intensity of the coloration. Approximately 90% of the carotenoids was canthaxanthin. No β-carotene was found in these eye tissues, although the patient had ingested a total dose of 11 g β-carotene besides 17 g canthaxanthin. This is in agreement with previous findings (Poh-Fitzpatrick and Barbera 1984). It must, however, be noted that tissue storage in formalin for several weeks was not ideal for chemical analysis and that possibly the β-carotene originally present has been eluted and/or degraded chemically, so it may no longer have been identifiable.

The canthaxanthin in the retina was present mainly in its all-*trans*-form. The *trans-cis* ratio was higher than in the agent ingested so that a preferred deposition of the all-*trans*-isomer may be assumed. Besides the retina, only the ciliary body contained measurable concentrations of canthaxanthin. We did not examine this tissue for crystals in frozen section and can, therefore, not decide whether the canthaxanthin is also bound to crystals in this part of the eye.

These results show that the name canthaxanthin retinopathy is justified. The term "carotenoid retinopathy" (Saraux and Laroche 1983; Tronnier 1984; Weber et al. 1985a, b) is too broad.

The question arises as to the pathogenesis of the crystalline deposits in the retina, which are obviously colored by canthaxanthin. The ring-shaped pericentral deposits of crystals are not related to the area of xanthophyll of the macula. Massive deposits of crystals are also situated far away from the area of the macula lutea.

According to their topographical distribution it is not possible to correlate the crystalline deposits definitely with a specific type of cell in the inner layers of the retina. The centrally more marked deposition might indicate a dependence on the ganglion cells. However, this assumption is contradicted by the frequency of crystals in the retinal periphery, where only a minimal number of ganglion cells is present. A dependence of the Müller cells must be considered. They are numerous foveally and perifoveally and, unlike the ganglion cells, their number diminishes less towards the periphery.

Comparison with other crystalline retinopathies, oxalosis, cystinosis, Bietti's crystalline, tapetoretinal dystrophy or tamoxifen retinopathy (Kaiser-Kupfer et al. 1981), is difficult because the position and distribution pattern of the crystals are different and/or no histological studies of the deposits are available.

In ultrastructural studies, it was not possible to determine the precise localization of the crystals in the not optimally fixed tissues. Certainly, the size of the large crystals makes an intracellular localization improbable. Their arrangement outside the nerve fibers and the formation of lacunae in the inner neuropil are suggestive of deposition in extracellular spaces that do not physiologically occur in the retina. We interpret the dissociation of the feet of Müller cells in the presence of intact basal membrane and the thinning of their branches as a pathological alteration in this specialized glia. Whether these alterations are caused by the large mass of crystals or are the expression of a primary atrophy of the cells, however, is undecided so far.

In our investigations, we were not able to elucidate the question of the immediate site of action and the pharmacological effects of canthaxanthin in the retina that might be responsible for the formation of the crystals colored with canthaxanthin. Since the crystalline deposits and therefore probably also the organic alterations demonstrated are irreversible, at least for a long period, it is ophthalmologically essential that very strict criteria be set for the indications and dosage of medication containing canthaxanthin.

Acknowledgements. We should like to thank Miss I. Pracht, Dr. G. Englert, Mr. W. Meister, and Mr. E. Glinz of the Central Research Units of F. Hoffmann-La Roche & Co. Ltd., Basle, for SMP, PMR and mass spectroscopy and for HPLC analysis; PD Dr. R. Guggenheim and Mr. G. Lüönd of the SEM Laboratory of the University of Basle for SEM and X-ray analysis; Mrs. R. van den Broek, Miss S. Locher, and Mrs. G. Bachmann for histotechnical, Mrs. S. Exinger for photographic, and Mrs. E. Wagner for editorial assistance. We are also grateful to Dr. A. Burette for supplying Fig. 1 as well as clinical information, to Dr. C. Malbrel for removing and delivering both eyeballs, and to Dr. H. Blancher for clinical information.

References

Bone RA, Landrum JT, Tarsis SL (1985) Preliminary identification of the human macular pigment. Vision Res 25:1531–1535

Boudreault G, Cortin P, Corriveau LA, Rousseau AP, Tardif Y,

Malenfant M (1983) Le rétinopathie à la canthaxanthine. 1. Etude clinique de 51 consommateurs. Can J Ophthalmol 18:325–328

Cortin P, Corriveau LA, Rousseau AP, Tardif Y, Malenfant M, Boudreault G (1982) Maculopathie en paillettes d'or. Can J Ophthalmol 17:103–106

Cortin P, Boudreault G, Rousseau AP, Tardif Y, Malenfant M (1984) La rétinopathie à la canthaxanthine. 2. Facteurs prédisposants. Can J Ophthalmol 19:215–219

Daicker B (1978) Die fleckige fettige Degeneration der Netzhautperipherie. Eine Form der „Schneckenspuren". Graefe's Arch Clin Exp Ophthalmol 205:147–155

Foos RY (1972) Vitreoretinal juncture, topographical variations. Invest Opthalmol 11:801–809

Franco JL, Adenis JP, Mathon C, Lebraud P (1985) Un nouveau cas de maculopathie en paillettes d'or. Bull Soc Ophthalmol Fr 85:1035–1037

Hennekes R, Weber U, Küchle HJ (1985) Über Canthaxanthinschäden der Netzhaut. Z Prakt Augenheilkd 6:7–9

Jakobiec FA (1982) Ocular anatomy, embryology and teratology. Harper & Row, Philadelphia, p 490

Kaiser-Kupfer MI, Kupfer C, Rodrigues MM (1981) Tamoxifen retinopathy. Ophthalmology 88:83–89

McGuiness R, Beaumont P (1985) Gold dust retinopathy after the ingestion of canthaxanthin to produce skin-bronzing. Med J Aust 143:622–623

Metge P, Maudirac-Bonnefoy C, Bellaube P (1984) Thésaurismose rétinienne à la canthaxanthine. Bull Mem Soc Fr Ophtalmol 95:547–549

Meyer JJ, Bermond P, Pournaras C, Zoganas L (1985) Canthaxanthin. Langzeiteinnahme und Sehfunktionen beim Menschen. Dtsch Apoth Z 125:1053–1057

Philipp W (1985) Carotinoid-Einlagerungen in der Netzhaut. Klin Monatsbl Augenheilkd 187:439–440

Poh-Fitzpatrick MB, Barbera LG (1984) Absence of crystalline retinopathy after long-term therapy with β-carotene. J Am Acad Dermatol 11:111–113

Puissant A (1984) La carotinodermie et la pilule à bronzer. Journée Ann Nutr Diet (Paris) 25:1–4

Ros AM, Leyon H, Wennersten G (1985) Crystalline retinopathy in patients taking an oral drug containing canthaxanthine. Photodermatology 2:183–185

Rousseau A (1983) Canthaxanthine deposits in the eye. J Am Acad Dermatol 8:123–124

Saraux H, Laroche L (1983) Maculopathie à papillottes d'or après absorption de canthaxanthine. Bull Soc Ophtalmol Fr 83:1273–1275

Tronnier H (1984) Zur Schutzwirkung von β-Carotin und Canthaxanthin gegen UV-Reaktionen der Haut. Z Hautkr 59:859–870

Weber U, Goerz G (1985) Augenschäden durch Carotinoid-Einnahme. Dtsch Ärztebl 82:181–182

Weber U, Goerz G (1986) Carotinoid-Retinopathie. III. Reversibilität. Klin Monatsbl Augenheilkd 188: 20–22

Weber U, Goerz G, Hennekes R (1985a) Carotinoid-Retinopathie. I. Morphologische und funktionelle Befunde. Klin Monatsbl Augenheilkd 186:351–354

Weber U, Hennekes R, Goerz G (1985b) Cartinoid-Retinopathie. II. Elektrophysiologische Befunde bei 23 Carotinoid-behandelten Patienten. Klin Monatsbl Augenheilkd 187:507–511

Received August 10, 1986 / Accepted January 26, 1987